IOSR Journal of Electrical and Electronics Engineering (IOSR-JEEE)
e-ISSN: 2278-1676,p-ISSN: 2320-3331, Volume 15, Issue 3 Ser. I (May – June 2020), PP 01-08
www.iosrjournals.org

Optimization Performance of PV System Based on Predictive Current Control

Dhaif Allah Hadi[1], PiWei[1*], Omar BusatiAlzain[2]
[1]*(Key Lab. of HV and EMC Beijing, Electrical & Electronic Engineering School,North China Electric Power University, R.P.China)*
[2] *(School of Control and Computer Engineering, North China Electric Power University, R.P.China)*

Abstract: *The electrical power generation based on the sun's rays through a series of solar cells linked together is considered as clean energy that reduces gas emissions are harmful compared to those produced by fossil fuels. Thus, lead to decrease the effects on the components of the environment. Also, the unknown impacts on the system behaviorwill inevitably affect the final response of the system, so it requires a more robust and effective control methodology. This paper presents the current control based the model predictive control (MPC) to generate optimal pulse of converter gates to handle the photovoltaic system (PV) unit based on maximum power point tracking (MPPT). The MPC has features that can offer stable regulation for an uncertainty effects during different dynamic conditions. The DC-DC boost converter based on the Fuzzy logic controller (FLC) is used to boost up and handle the photovoltaic voltage to satisfy the total efficiency by applying the MPC-current control on the AC inverter. In this study, the MPC is used to control the system in order to meet suitable performance according to the minimization procedures for the optimization problem. MATLAB is used to achieve the simulation results and show that, the MPC is more efficient and gives better output performance comparing with PI and FLC control.*

Key Word: Model predictive control; Fuzzy logic control; Photovoltaic integration system; PI controller

---

Date of Submission: 27-04-2020 Date of Acceptance: 10-05-2020

I. Introduction

The solar refinery concept is to satisfy growing electricity desires, whilst restricting greenhouse gas emissions over the approaching decades, energy capacity on a big scale will want to be supplied from renewable sources, with solar predicted to play a principal position. At present, the manufacture of photovoltaic (PV) energy is considered as pivot point and It is one of the first energy consumed in the world. However, the highest energy used is dependent on fossil fuels that cause many environmental problems compared to cleaner energy alternatives. As well, the last type which enhances the use of the cheapest energy and the possibility of transporting it to remote locations [1]. Conventional PV systems employ series-connection of PV panels, organized into strings, a good way to offer a voltage-stack at the center of grid-tied inverters.An emergence of The allotted maximum power point tracking (MPPT) of PV structures, may lead to increase the extent of system performance capability.This observes makes specialty of the various implementations of these architectures and offers an in-intensity analysis concerning to their boundaries of power. [2. Amongst those, MIC perception has become the most current technique for grid-tied PV tool improvement within the marketplace and it will likely be a tendency for destiny solar PV deployment, due to its superior advantages including the low value of production amount, enormous performance, simpler installation, and increase power harvest [3]. The industrial MIC structures are extensively used in a single phase allotted PV era with a electricity range of a 105-400 w and input dc voltage is about 20-45 v. Since, the low PV voltage desires to be boosted into utility grid voltage, several MIC topologies have been used in conversion stages and the design critical had been studied and offered within the literature [2, 4]. Micro inverters when its compared to different energy conversion systems for pv applications, many advantages has been harvested, lifetime and reliability. For that reason a lot interest has been raised in this subject matter in latest years. Because using fly back has many drawback such as high voltage strain on semiconductor and electromagnetic (EM) noise. The proposed converter consequences in unmarried level power conversion with decreased passive additives, low voltage pressure and decreased EM noise [5]. This structure will reduce the cost per watt, improve machine reliability, and eliminate the single-factor failure. Assuming further expansion of the 3-segment grid-tied MIC gad-get into big-scale PV installation it might be required for micro-inverters to be equipped with low voltage ride through (LVRT) capability a good way to satisfy the Upcoming necessities under fault situations. Previously, analyzed control schemes targeted on LVRT enhancement of the voltage source. Converter (VSC)-primarily based MIC structures, which are primarily based on the concept of *d-q* rotating frame with classical linear proportional-integral (PI) regulators and pulse-width space vector modulation (PWSVM) [6, 7]. Unlike VSC, the unbalanced grid voltage of the PV inverter module, the controller destine through active and reactive power as the controller to obtain LVRT control studied in the literature [9, 10]. The property of a single power stage is preserved and the input DC side voltage of the inverting system is less than the output of grid voltage, which perfectly suits the property of a wide output voltage range in PV cells. [11]. This paper implies on the application of the three-phase voltage source converter (VSC)with PV grid-tied system for the three-phase grid, which is connected with PV farm in this paper the power of solar farm is 100KW and the voltage 500VDC. A FLC and predictive control strategy are applied to the boost-converter and Ac inverter to make the PV voltage stable. Moreover, MIC provided a balanced grid voltage under disturbances, with active and reactive power. The control objectives are expressed as function. During each sampling interval, the fitness function is minimized using the actual measurements and predicted values for given switching states, which are then applied to the VSC-based MIC directly.

II. System Configuration And Modeling

The system scheme of PV panel constructed based on three phase MICs can be seen in Fig.1. A three-phase MIC-CSC is connected to each PV cell. The voltage output of MIC for each PV cell is connected to the grid side voltage. In fact, each MIC with its cell works separately even if the other MIC is unsuccessful in operation that has no effect among others. A three-level bridge unit based on power electronics devices is selected. Series RC snubber circuits are tied in parallel with each switch unit. A series inductor Ldc play important rule as storage element for the energy, which creates the DC link bus. The direct voltage of PV panel is controlled by using the boost-fuzzy control. Then the voltage inverted by CSC, which directly connected to the grid transformer via LC filter.

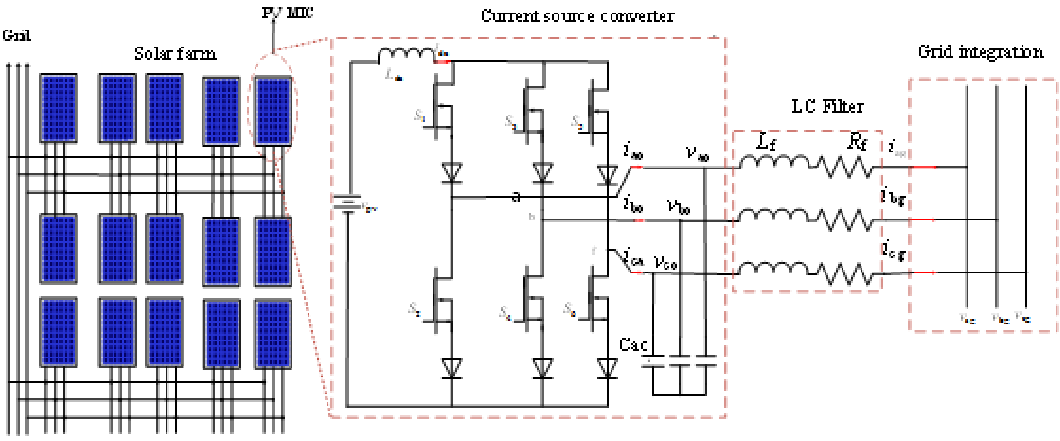

Fig.1. Block scheme for PV system

2.1 CSC-based MIC modeling design

In this article, both types of power (Active power and reactive) are considered to be controlled by using the grid currents modeling at the synchronous reference frame. For a three-phase CSC, 9 switching combinations states are generated, i.e., three charging operating statuses and six discharging operating statuses, which are presented as in Table I. At any switching period, only two active switches actions, one of the upper MOSFETs (*s1*,*s3*,*s5*) and the secondfor the lower MOSFETs (*s4*,*s6*,*s2*) to continue a flow pass through an inductor current, i.e. The dc-link current are affecting by 9 possible switching position for the CSC-based MIC unit as shown in Fig.1

Table .1 Swathing states of voltage for three phase inverter

S11	S21	S31	Vab	Vbc	Vca
0	0	0	0	0	0
0	0	1	0	Vdc	Vdc
0	1	0	Vdc	Vdc	0
0	1	1	Vdc	0	Vdc
1	0	0	Vdc	0	-Vdc
1	0	1	Vdc	Vdc	0
1	1	0	0	Vdc	- Vdc

1	1	1	0	0	0

The *d-q* grid current formula can be expressed in terms of output voltages of converter, grid voltages and filter impedance as

$$\begin{cases} L_f \dfrac{di_{dg}}{dt} + R_f i_{dg} - L_f w_g i_{qg} = V_{do} - V_{dg} \\ L_f \dfrac{di_{dg}}{dt} + \;\; R_f i_{dg} + L_f w_g i_{qg} = V_{qo} - V_{qg} \end{cases} \qquad (1)$$

Where *Lf* and *Rf* are the inductance and impedance of the grid side filter. *Vdo*, *Vqo*, *Vdg*, and *Vqg*are *dq*-axis voltage items and *idg* and*Iqg* are the grid current items.*Wg*is angular frequency of grid. the capacitor currents can be obtained based on inverteroutput voltage:

$$\mathrm{ide} = -\omega_g C_f V_{qo} \; and \;\; iqe = \omega_g C_f V_{do} \qquad (2)$$

Therefore, the inverter current and voltage:

$$\begin{aligned} V_{do} &= 1/\,w_d C_f \,.\left(i_{qo} - i_{qg}\right) \\ V_{qo} &= 1/\,w_d C_f \left(i_{dg} - i_{do}\right) \end{aligned} \qquad (3)$$

From (1) (2)& (3), thecontinuous time state spaceequationof the system based on the dq-grid current can be written as:

$$\frac{d}{dt}\begin{bmatrix} i_{dg} \\ i_{qg} \end{bmatrix} = K\begin{bmatrix} i_{dg} \\ i_{qg} \end{bmatrix} + L\begin{bmatrix} i_{d0} \\ i_{q0} \end{bmatrix} + M\begin{bmatrix} U_{dg} \\ U_{qg} \end{bmatrix} \qquad (4)$$

Where K, L and M are matrix of dynamic factors

$$K = \begin{bmatrix} \dfrac{-R_f}{L_f} & \dfrac{w_g^2 L_f C_f - 1}{w_g L_f C_f} \\ \dfrac{w_g^2 L_f C_f + 1}{w_g L_f C_f} & \dfrac{-R_f}{L_f} \end{bmatrix}, \quad L = \begin{bmatrix} 0 & \dfrac{1}{w_g L_f C_f} \\ \dfrac{-1}{w_g L_f v_{DC}} & 0 \end{bmatrix}, \quad M = \begin{bmatrix} \dfrac{-1}{L_f} & 0 \\ 0 & \dfrac{-1}{L_f} \end{bmatrix}$$

2.2 Discrete-time of current based MPC

For the digital implementation of MPC algorithm, Discrete-time model of the system is suggested. Microprocessor based hardware helps in the real-time implementation of such models. The discrete-time system describes the *dq*-axis of the gridcurrents can be obtained from (3) for the one-step predictionas:

$$\begin{bmatrix} i_{dg}^p(k+1) \\ i_{qg}^p(k+1) \end{bmatrix} = X_A\begin{bmatrix} i_{dg}(K) \\ i_{qg}(K) \end{bmatrix} + X_B\begin{bmatrix} i_{do}^e(k) \\ i_{qo}^e(k) \end{bmatrix} + X_C\begin{bmatrix} U_{dg}(K) \\ U_{qg}(K) \end{bmatrix} \qquad (5)$$

Where, $X_A = e^{ATs}, X_B = A^{-1}(X_A - I) = A^{-1}(X_A - I)C$

Where*idg*(*k*), *iqg*(*k*), *vdg*(*k*), and *vqg*(*k*) are the *dq*-axis ofthe measured grid currents and voltages while Ts is controllersampling time.The discrete sequences of the converter output currents in*dq*-axis reference frame can be estimated from switchingsignals*S1* (k) -*S6*(k) and dc-link inductance current measurement,*itc* (*k*), are expressed as:

$$\begin{bmatrix} i_{do}^e(k) \\ i_{qo}^e(k) \end{bmatrix} = K.i_{dc}^m(k)\begin{bmatrix} S_1(k) - S_4(k) \\ S_3(k) - S_6(k) \\ S_5(k) - S_2(k) \end{bmatrix} \qquad (6)$$

Where K is the *abc/dq* transformation matrix as:

$$K = \frac{2}{3}\begin{bmatrix} \cos\cos\theta_g(k) & \cos(\theta_g(k) - \frac{2\pi}{3}) & \cos(\theta_g(k) - \frac{4\pi}{3}) \\ -\sin - \sin\theta_g(k) & -\sin(\theta_g(k) - \frac{2\pi}{3}) & -\sin(\theta_g(k) - \frac{4\pi}{3}) \end{bmatrix}$$

Where, *Bg*(*k*) is grid voltage angle, which can be obtained byan phase-locked loop (PLL).

The one-step prediction methodology is often used to simplifyanalysis and digital implementation computations. However, in the real-time implementation, the computational delay produced by the digital signal processor needs taking consideration[14]. Thus, the discrete time equation (6) is shifted one step forward, i.e., (*k+2*) prediction.To save computational effort, the same estimated converter currents*ido*(*k*) and *iqo*(*k*), are used in *k+2* prediction ofgrid currents [14]. The discrete-time model for the two-stepprediction of grid currents is as follows

$$\begin{bmatrix} i_{dg}^{p}(k+2) \\ i_{qg}^{p}(k+2) \end{bmatrix} = X_A \begin{bmatrix} i_{dg}^{p}(k+1) \\ i_{qg}^{p}(k+1) \end{bmatrix} + X_B \begin{bmatrix} i_{do}^{e}(k) \\ i_{qo}^{e}(k) \end{bmatrix} + X_C \begin{bmatrix} U_{dg}(K+1) \\ U_{qg}(K+1) \end{bmatrix} \qquad (7)$$

Where,*idg* (k+2) and $i_{qg}(k+2)$ are the predicted grid currents in (k+2) state using 9 possible switching combinations. For asmall enough sampling time and to save computational efforts,it is possible to consider *Vdg* (*k+1*),…,*Vdg* (*k*) and *Vqg*(*k+1*),…,*Vqg*(*k*). From (6) and (7), the future behavior of the *d-q* components of the grid current which are related to the converter switching signals can be obtained based on the actual measurements and estimated converter currents. The optimal switching state can be selected among the 9 switches.

2.3 Strategy of CSC control based on MIC

The finite control set of predictive controller is an optimization control system; it gives the switching singles directly to the converter without any difficulties in modulation technique such as SVM or PWM. The presented control system of the converter based on MIC gives an exact amount of power in terms of active and reactive based on productive values. Actually, in steady-state operation and also a proper percentage of reactive power for low voltage through regulation during the transient process. Fig.2shows the current sources converter control, which mainly has two sections productive block and command block.

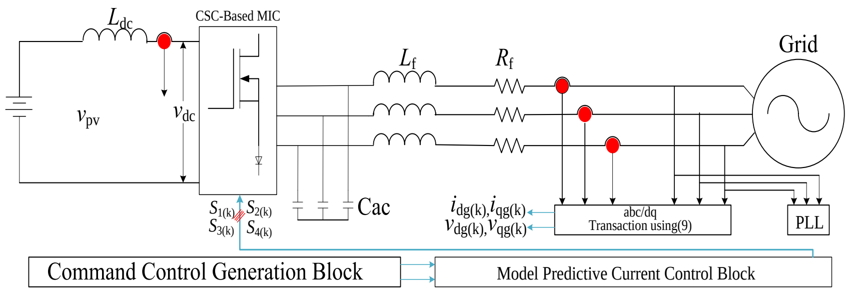

Fig.2.Block scheme for proposed control system

The references of control variables during steady and transient states are presented.The *dq*-axis grid current reference is generated by a method which is similar to the classical voltage-oriented control.

1- Steady-State process: In this part, the main objectives of MIC-based converter are two of the main variable control. The first is to offer certain values to the active power and direct current toward the network. Therefore, the dq-axes of the current can be generated based on the transformation methods of the AC current. Assuming that 1 per unit scale is the full rate of current values. Thus, the power by watt of the network can be written as:

$$P_g^*(k) = \sqrt{S_{MIC}^2 - Q_g^*(k)^2} \qquad (8)$$

Where, S_{MIC} is the apparent rated power of the converter.

The reference current based on DC-bus is evaluated based on active power $P_g^*(k)$. The current based DC-bus is identicalto real measured current, so the difference between these two current values is fed throughout PI controller to yield the reference voltage of DC-bus $V_{dc}^*(k)$. The DC–link voltage and current toward the PV panel side V_{pv} and the inductance voltage can be described as:

$$VL_{de}(k) = Vpv(k) - Vde(k) \qquad (9)$$

Assume that to find reference current: free of loss,and the power of PV is equal the DC–link power. Therefore, the grid current is:

$$i_{dg}^*(k) = \frac{P_g^*(k)}{1.5v_{dg}(k)} = \frac{v_{dc}^*(k)\, i_{dc}(k)}{1.5v_{dg}(k)} \qquad (10)$$

2- Transient-State process: Nowadays, a lot of systems are improving their interlinking regulation such as LVRT for medium and large scale PV power Plant standard. There are many examples for that, but there real on is Danish system [15].

$$i_{dg}^*(k) = \sqrt{I_n^2 + i_{dg}^*(k)^2} \quad (11)$$

2.3.1 Model predictive current control design

The design model is presented in Fig.2 by using two control methods FLC and MPC for the DC boost and AC converter respectively. According to Fig. 3,the future grid current valueat (*k+2*) is predicted through the 9 switchesassociations which are generated by the MIC-CSC by using (6) and (10). The estimated current references at the instant *k+2* are needed todesign the MPC strategy. Thus, the obtained reference signals at*kth* instant are destined to *k+2* instant. When the narrow sampling time *Ts*< 20µs considering *i*g*(*k+2*) =*i*g*(*k*). However, *Ts*> 20µs, theLagrange series extrapolation can be used [l3]

$$i_g^*(k+2) = 6i_g^*(k) - 8i_g^*(k-1) + 3i_g^*(k-2) \qquad (12)$$

The predicted currents of the grid *idg*(k + 2) and *iqg* (k + 2) arematched with related reference values *i*dg* (*k+2*) and *i*g* (*k+2*), in a *d-q*reference frame using a cost function *f*, as following

$$f = i_{dg}^*(k+2) - i_{dg}^p(k+2)^2 + i_{qg}^*(k+2) - i_{qg}^p(k+2)^2 \ (13)$$

The goal of the cost function based PQ algorithm is optimizing the*f* value to close around zero. According to this approach, the optimal switches signals in the past iterations are used to estimate the control signals at each sample instant.

III. Simulations Results Analysis

The PV model based on power grid simulation is examined with the proposed strategy FLC-MPC with a set of rated values for the PV and proposed controller. Where, Table1 shows the parameters and rated values that were used in the proposed modeling under study and their definition

3.1 Design of FLC and MPC controller for PV grid-connected

The proposed strategy FLC-MPC controller has been designed for the PV connected with the power network. The DC-DC boost converter is controlled by FLC controller. And the MPC controller is designed to handle the DC-AC converter based on the two ahead current sequences. The simulation results have been carried out by using MATLAB-SIMULINK. Where, the FLC is built as Mamdani model has a fuzzy rules number equal 49 rules, two inputs as error *E* and change of error *CE*, one output U, triangular shape of membership inference set and centroid propagation type. The FLCgenerated the control signals as pulses for DC/DC converter switches.

In the MPC controller, theinput horizon is 4, prediction horizon is 11, the input constraints specified as general formula $U_{\min} < U < U_{\max}$ the quadratic program algorithm is used to find the optimal switches converter signals depend on the general formula of the current state space model and theVSI. The simulation outcomes are presented and show the validation of the MPC based on MIC. To be more precise the dynamic preference of the model is shown better overshooting time and peak values as compared to other models. The values of the dynamic performance of productive controller are listed in Table -II.

Table-2 Dynamic prosperities of differences control approaches

		PI-PI	*PI-FLC*	*FLC-MPC*
Over shoot		*16%*	*16.2%*	*15.4%*
Peak time		*0.128*	*0.123*	*0.04*
Settling time		*0.17*	*0.2*	*0.158*
THD	***Volt***	*8.78%*	*9.34%*	*3.72%*
	Current	*7.92%*	*7.82%*	*3.57%*

Fig.3(a) represents the radiation behavior assumed to be 1000 within 0-0.59 sec then declines by a slope to 252 and by the same increased slop return to 1000 at 1.7 sec. Also in Fig.3 (b), the temperature on the panel is assumed to be 25 C° from 0 to 2 sec then the slop increasing to 75C° until end of time.In Fig.3 (c)the dynamic performance of the proposed FLC-MPC strategy is studied for the system power signal. The shape of power response is began from 96.56 KW over 0.59 sec then decrease its slop to 23.05 KW, after 1.11 sec is spent the power signal decrease slop to 96.56 KW according to the radiation and temperature behavior. Also, Fig. 5 shows that, when the temperature signalat 75C^o the power signal response is decreased to 95.9KW. The proposed FLC-MPC strategy gave good satisfactory power signal with 8.56% as ratio overshooting, 0.10 sec rise time, 0.11 sec peak time and 0.17 sec settling time at the first growth of the response.

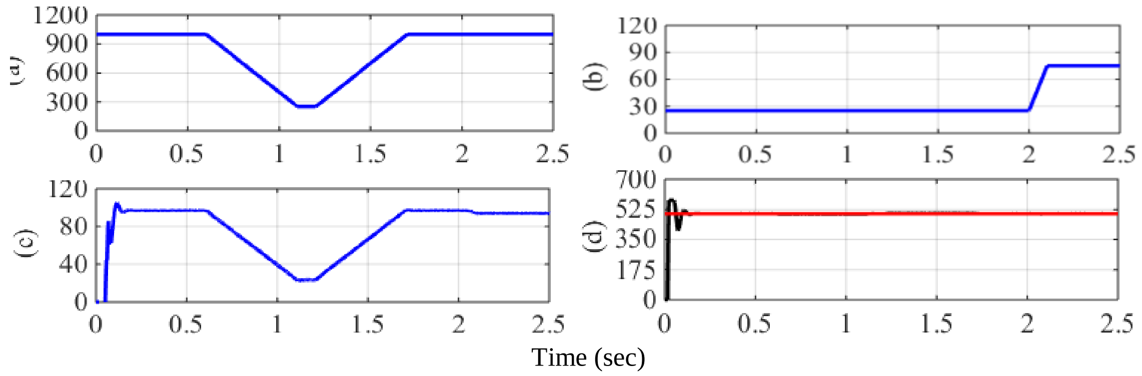

Fig.3, the dynamic response of PV based FLC-MPC (a) radiation signal (b) temperature signal (c) power

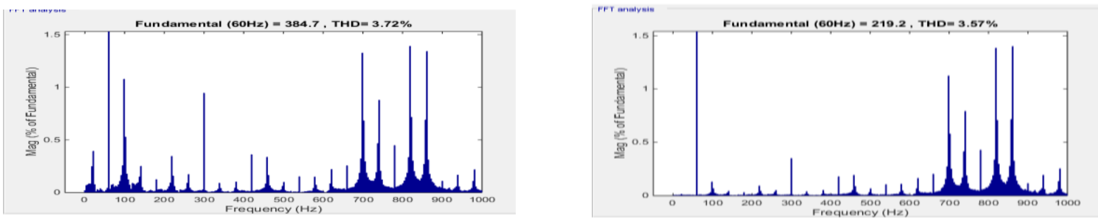

response (d) DC voltage response

Fig.4. The THD for the AC voltage and current based on FLC-MPC respectively.

In Fig.3 (d) the FLC-MPC strategy is introduced the DC-link voltage of capacitor signal. The shape of DC voltage response is trackingthe reference voltage which is set to 500 V for all simulation time. The proposed FLC-MPC strategy gave good tracking response for the DC voltage signal with 15.38% as ratio overshooting, 0.09 sec rise time, 0.03 sec peak time and 0.18 sec settling time at the first growth of the response. The THD is calculated by using FFT analysis to a measure voltage and current with considering 17 cycles and frequency 60Hz along 1000 Hz frequency range to obtained the low percentage of total harmonic distortion about 3.72% and 3.57% , respectively as shown in Fig. 4.

3.2 Current control approaches based on FLC-PI

Design of FLC-PI Controller as a comparative method with the proposed approach for PV Grid-Connected:FLC and PI controller has been designed to control the boost converter and AC inverter for the PV connected with the power network respectively. The FLC parameters are set as previous values and PI controller parameters are set as Kp=2.1, and Ki=0.6.

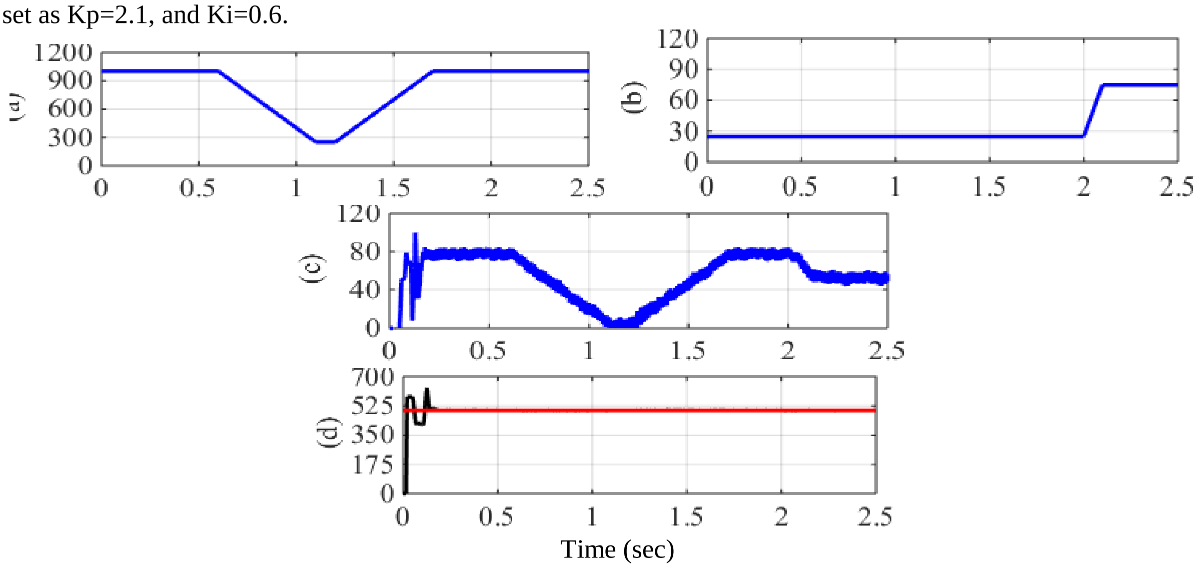

Fig.5, the dynamic response of PV based FLC-PI(a) radiation signal (b) temperature signal (c) power response (d) DC voltage response

In Fig.5 (c), for the same conditions of previous tests, the power response is began from 94.88 KW over 0.22 sec then decreases its slop to11.07 KW after 1.1 sec is spent the power signal decreases slop to 94.88

KW according to the radiation and temperature behavior.

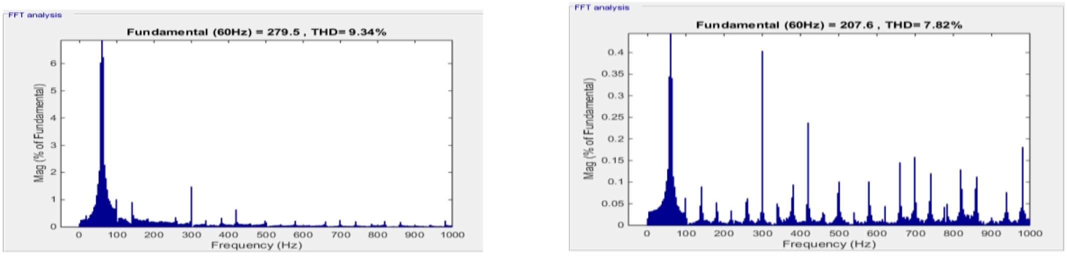

Fig.6. The THD of AC voltage and current based on FLC-PI

Also, Fig.5 (c) shows that, when the temperature signals to 75 C^o the power signal response is decreased to 70 KW. The proposed FLC-PI strategy give the power signal with 11.29% as ratio overshooting, 0.14 sec rise time, 0.15 sec peak time and 0.23-sec settling time at the first growth of the response.

In Fig.5 (d) the FLC-PI strategy gave a good tracking response for the DC voltage signal with 28.8% as ratio overshooting, 0.13 sec rise time, 0.14 sec peak time and 0.19-sec settling time at the first growth of the response. The total harmonic distortion for AC voltage andcurrent are 9.34% and 7.82%, respectively as shown in Fig. 6.

3.3 Current Control approaches based on PI-PI

Design of PI-PI Controller as a comparative method with the proposed approach for PV Grid-Connected: FLC and PI controller has been designed to control the boost converter and AC inverter for the PV connected with the power network respectively. The PI parameters are set as previous values.In Fig.7 (c) for the same conditions of previous tests, The shape of power response began from 93 KW over 0.19 sec then decreases its slop to21.43 KW after 1.11 sec is spent the power signal decreases slop to 79.88 KW according to the radiation and temperature behavior. Also, Fig.7 (c) shows that when the temperature signals to 75 Co the power signal response is decreased to 80 KW. The proposed PI-PI strategy give the power signal with 27.58% as ratio overshooting, 0.14 sec rise time, 0.15 sec peak time and 0.20-sec settling time at the first growth of the response.In Fig.7 (d), the DC voltage response is tracking the reference voltage which is set to 500V. The proposed PI-PI strategy gave good tracking response for the DC voltage signal with 32.28% as ratio overshooting, 0.017 sec rise time, 0.14 sec peak time and 0.19-sec settling time at the first growth of the response.The total harmonic distortion for AC voltage andcurrent are 8.78% and7.92%, respectively as shown in Fig. 8.

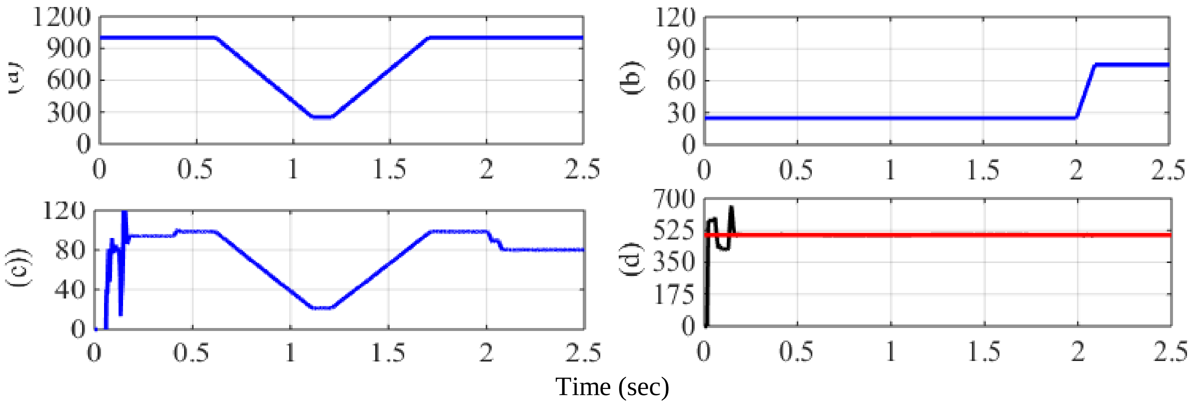

Fig.7, the dynamic response of PV based PI-PI (a) radiation signal (b) temperature signal (c) power response (d) DC voltage response

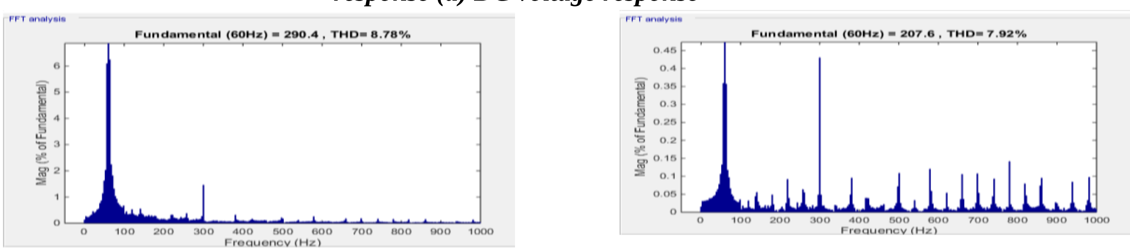

Fig.8. The THD of AC voltage and current based on PI-PI

IV. Conclusion

This paper presents the current control based the model predictive control (MPC) to generate optimal pulse of converter gates to handle the photovoltaic system (PV) unit based on maximum power point tracking (MPPT). The MPC has features that can offer stable regulation for an uncertainty effects during different dynamic conditions. The DC-DC boost converter based on the Fuzzy logic controller (FLC) is used to boost up and handle the photovoltaic voltage to satisfy the total efficiency by applying the MPC-current control on the AC inverter.As mentioned in previous sections, the optimal signals of Ac converter gates are producing from the current MPC controller and DC-DC enabling signal is producing from the FLC controller, then all the responses of the proposed control are compared with traditional PI-PI and FLC-PI for the DC-DC converter and the AC converter respectively.According to the simulation results, the FLC-MPC has better tracking performance than PI-PI and FLC-PI controller with smaller overshoots and quicker response for the reference signal and the required characteristics. The FLC-MPC has a low total harmonic distortion than the FLC_PI and PI-PI controller. These can directly result in less ripple of the dynamic responses. Thus, unit fatigue and its associated maintenance cost caused by such maneuvering actions obviously decreased comparing with the FLC-PI and PI-PI strategy.

Acknowledgement

This work was supported in part by the National Natural Science Foundation of China under Grant 51877083 and in part by the Fundamental Research Funds for the Central Universities under Grant 2018MS004.

References

[1]. Tuller, Harry L. "Solar to fuels conversion technologies: a perspective." Materials for renewable and sustainable energy6, no. 1 (2017): 3. J. Clerk Maxwell, A Treatise on Electricity and Magnetism, 3rd ed., vol. 2. Oxford: Clarendon, 1892, pp.68-73.

[2]. L. Chen, A. Amirahmadi, Q. Zhang, N. Kutkut, and I. Batarseh, "Design and implementation of three-phase two-stage grid-connected module integrated converter," Power Electronics, IEEE Transactions on, vol. 29, no. 8, pp. 3881-3892, Aug 2014..

[3]. Khan, O., and W. Xiao. "Review and qualitative analysis of submodule-level distributed power electronic solutions in PV power systems." Renewable and Sustainable Energy Reviews76 (2017): 516-528.

[4]. Y. Zhou, L. Liu, and H. Li, "A high-performance photovoltaic moduleintegrated converter (mic) based on cascaded quasi-z-source inverters (qzsi) using eganfets," Power Electronics, IEEE Transactions on, vol. 28, no. 6, pp. 2727-2738, June 2013.

[5]. Palma, L. "Push-pull based single stage PV microinverter for grid-tied modules." In 2016 International Symposium on Power Electronics, Electrical Drives, Automation and Motion (SPEEDAM), pp. 884-888. IEEE, 2016.

[6]. M. Castilla, J. Miret, J. Matas, L. Garcia de Vicuna, and J. Guerrero, "Control design guidelines for single-phase grid-connected photovoltaic inverters with damped resonant harmonic compensators," Industrial Electronics, IEEE Transactions on, vol. 56, no. 11, pp. 4492-4501, Nov 2009.

[7]. Castilla, Miguel, JaumeMiret, José Matas, Luis García De Vicuña, and Josep M. Guerrero. "Control design guidelines for single-phase grid-connected photovoltaic inverters with damped resonant harmonic compensators." IEEE Transactions on industrial electronics 56, no. 11 (2009): 4492-4501.

[8]. Chen, Xia, Yanwei Cui, Xinru Wang, and Shuangshuang Li. "Research of low voltage ride through control strategy in photovoltaic (PV) grid." In 2017 Chinese Automation Congress (CAC), pp. 5146-5150. IEEE, 2017.

[9]. N. Kalaiarasi; K Charishma, "Design of Grid connected Photovoltaic Inverter with Resonant Harmonic Compensator", International Jorum of Science and Research (IJSR) volume 4 lssue4, April 2015, 1004-1008.

[10]. Qin, Zian, DeshangSha, and Xiaozhong Liao. "A three-phase boost-type grid-connected inverter based on synchronous reference frame control

[11]. In 2012 Twenty-Seventh Annual IEEE Applied Power Electronics Conference and Exposition (APEC), pp. 384-388. IEEE, 2012.

[12]. Chen, Yang, and KeyueSmedley. "Three-phase boost-type grid-connected inverter." IEEE Transactions on Power Electronics 23, no. 5 (2008): 2301-2309.

Dhaif Allah Hadi., etal. "Optimization Performance of PV System Based on Predictive Current Control." *IOSR Journal of Electrical and Electronics Engineering (IOSR-JEEE)*, 15(3), (2020): pp. 01-08.